===== CONDENSED =====
===== MATTER =====

Toroidal Configuration of a Cholesteric Liquid Crystal in Droplets with Homeotropic Anchoring

M. N. Krakhalev[a, b, *], V. Yu. Rudyak[c], A. P. Gardymova[b], and V. Ya. Zyryanov[a]

[a] Kirensky Institute of Physics, Federal Research Center KSC, Siberian Branch, Russian Academy of Sciences,
Krasnoyarsk, 660036 Russia

[b] Institute of Engineering Physics and Radio Electronics, Siberian Federal University, Krasnoyarsk, 660041 Russia

[c] Faculty of Physics, Moscow State University, Moscow, 119991 Russia

*e-mail: kmn@iph.krasn.ru

Orientational structures formed in cholesteric droplets with homeotropic surface anchoring have been studied by means of polarization optical microscopy and computer simulations. It has been found that, when the ratio of the size of droplets to the pitch of a cholesteric helix ranges from 1.4 to 2.9, an axisymmetric toroidal cholesteric structure is formed with a topological linear defect in the form of an equatorially located surface ring. The features of the toroidal structure in cholesteric droplets and their optical textures for various observation schemes are examined in detail.

The director field **n** (unit vector oriented along the favorable direction of long axes of molecules) in cholesteric liquid crystals in a free state forms a helical structure characterized by the intrinsic pitch of the helix p_0 at which the director is rotated by an angle of 2π. The interaction of cholesteric liquid crystals with bounding surfaces is responsible for the formation of diverse structures depending on boundary conditions and the ratio of the pitch of the helix to the thickness of a cholesteric liquid crystal layer [1]. When a cholesteric liquid crystal is located in a confined cavity, the geometry of the cavity imposes additional conditions on the structure of the liquid crystal in addition to the above factors [2, 3]. In turn, a structure formed in such cavities affects the optical [4−7], photomechanical [7, 8], thermomechanical [9, 10], hydrodynamic (*microswimmer*) [11], etc., properties of cholesteric liquid crystal droplets.

In the case of tangential anchoring, defects with the total surface topological charge equal to the Euler characteristic of the surface (+2) are formed on the surface of droplets. In particular, a twisted bipolar configuration [12−14] and a structure with a χ^{+2} dislocation or a χ^{+1} diameter dislocation [12−18] can be formed depending on the ratio of the pitch of the helix to the diameter of the droplet. The bipolar configuration is formed in the case of a relatively large pitch of the helix; as the pitch of the helix decrease, surface point defects approach each other and the structure is

finally transformed into the configuration with the χ^{+2} dislocation [12, 14].

In the case of homeotropic anchoring, helicoidal ordering or/and boundary conditions should be disturbed on the surface of the droplet. As a result, structures with various combinations of point and linear defects in the bulk and near the surface [19, 20], a structure with a linear surface defect in the form of double twisted helix [15, 21, 22], a structure of nested cups [15], and other layered structures [23, 24] can be formed in droplets. The formation of structures with point defects in the bulk makes it possible, on one hand, to keep the homeotropic orientation on the entire surface of the droplet and, on the other hand, to implement twisting of the director in the bulk. The number and type of point defects depend on the ratio of the diameter of the droplet d to the intrinsic pitch of the helix p_0; in this case, the law of conservation of the total topological charge of defects is satisfied [19, 20]. At relatively large ratios d/p_0, layered structures without point defects are observed more frequently, which promotes a lower twist strain of a cholesteric liquid crystal (helicoid). In particular, the pitch of the helix formed in droplets with the bipolar helix axis distribution in the structure at $d/p_0 > 5$ is close to the intrinsic pitch of the helix p_0 [25]. In this case, a twisted ring defect appears on the surface of the droplet [22]; this defect makes it possible to keep the homeotropic orientation of the director on almost the entire surface of

the droplet and simultaneously to implement a twisted structure in the bulk.

In this work, we perform experimental and computer simulation studies of the orientational structure in cholesteric liquid crystal droplets that is formed under the homeotropic boundary conditions for ratios d/p_0 between values characteristic of the twisted radial structure with a point defect and a configuration with the bipolar helix axis distribution.

Experimental studies were carried out for cholesteric liquid crystals based on the E7 nematic liquid crystal (Merck) doped with 3.0 wt % cholesteryl acetate (Sigma Aldrich). The intrinsic pitch of the helix at this concentration is $p_0 = 5.5$ μm [25]. To obtain droplets with the homeotropic anchoring, the cholesteric liquid crystal was dispersed in poly(isobutyl methacrylate) (Sigma Aldrich). Composite film samples were fabricated by the TIPS technology [26] with the weight ratio cholesteric liquid crystal : poly(isobutyl methacrylate) = 60 : 40. The size of droplets d (visible diameter of droplets in the sample plane) was determined by the cooling rate and varied in the range of 2−30 μm. The studies were performed with an Axio Imager.A1m (Carl Zeiss) polarizing optical microscope at a temperature of $t = 25°C$.

The computer simulations were performed within the Frank elastic continuum theory including the elastic energy of distortion of the director field, the surface energy of interaction of the liquid crystal with the interface, and the energy of disclinations [27]:

$$F = \int_V \left(\frac{K_{11}}{2}(\text{div}\mathbf{n})^2 + \frac{K_{22}}{2}(\mathbf{n} \cdot \text{curl}\mathbf{n} + q_0)^2 \right.$$

$$\left. + \frac{K_{33}}{2}[\mathbf{n} \times \text{curl}\mathbf{n}]^2 \right)dV + \frac{W}{2}\int_\Omega [1 - \cos^2\gamma]d\Omega \quad (1)$$

$$+ F_{\text{def}}.$$

Here K_{11}, K_{22}, and K_{33} are the splay, twist and bend elastic constants, respectively; $\mathbf{n}$ is the director field in the droplet; W is the energy of the surface anchoring per unit area; γ is the angle between the director and normal to the surface; $q_0 = 2\pi/p_0$ is the equilibrium cholesteric twist wavenumber; and F_{def} is the total energy of point and linear defects. The optimization of the director field was performed by the Monte Carlo simulated annealing method with the Metropolis criterion. The calculations were performed for a spherical droplet on a $48 \times 48 \times 48$ grid with the ratio $K_{11} : K_{22} : K_{33} = 1 : 0.6 : 1.25$, which corresponds to the E7 nematic mixture, and the linear energy density of disclinations $f_{\text{core}}^{\text{line}} = 2.75K_{11}$. The surface anchoring energy was specified through the dimensionless parameter $\mu = WR/K_{11} = 200$, which corresponds to strong anchoring (here and below, R is the radius of the droplet). The equilibrium pitch of the cholesteric helix was taken to be $p_0 = 5.5$ μm.
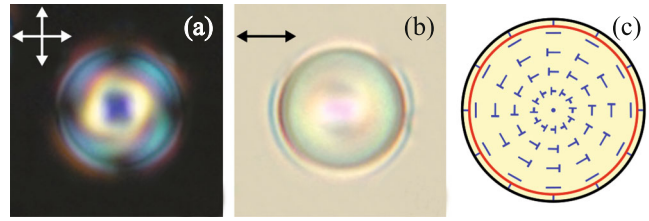

Fig. 1. (Color online) Photographs of a droplet with the toroidal structure of the cholesteric liquid crystal where the axis of symmetry of the droplet is perpendicular to the sample plane (a) in the scheme of crossed polarizers and (b) without analyzer. (c) Schematic of the director lines in the central cross section of the droplet. Here and in the other figures, double arrows indicate the directions of polarizers and the red line denotes the surface ring defect. The diameter of the droplet is 11 μm and the intrinsic pitch of the cholesteric helix is $p_0 = 5.5$ μm.

Under homeotropic boundary conditions, a radial configuration of the director is formed in the nematic droplet with a bulk hedgehog point defect at the center of the droplet [26]. In cholesteric droplets with small ratios d/p_0, an untwisted radial configuration is also formed [28]. In the system under study, such a structure is observed in droplets with diameters smaller than 3 μm. With an increase in the size of droplets, the radial structure is twisted and, simultaneously, the point defect is shifted from the center of the droplet. In droplets with diameters equal to and larger than 5 μm ($d/p_0 \cong 1$), the point defect is located near the boundary of the droplet. Such a picture can be observed in individual droplets with diameters up to 15 μm ($d/p_0 \cong 2.7$).

Droplets with diameters in the range of 8 to 16 μm demonstrate an axisymmetric configuration (Fig. 1), which is much similar to the toron structure in the planar cholesteric layer [29]. Such a toroidal cholesteric configuration in droplets includes a surface ring defect whose plane coincides with the central cross section of the droplet and is perpendicular to the axis of symmetry of the droplet. This is clearly seen when the axis of symmetry of the droplet lies in the sample plane (Fig. 2). The feature of the toroidal configuration of the cholesteric droplet is that the total rotation of the director along the diameter for any direction in the plane of the ring defect (in the equatorial cross section of the droplet) is π and is independent of droplet size. This is manifested in the optical texture as the absence of additional lines associated with the lensing effect.

The calculations confirm that the toroidal configuration of the director field of the cholesteric liquid crystal is stable in the indicated size range (Fig. 3). The structure corresponding to the global energy minimum is characterized by a high degree of axial symmetry (Fig. 3a). A ring defect is located on the surface in the equatorial cross section of the droplet. To analyze the topology of the resulting structure in more detail,
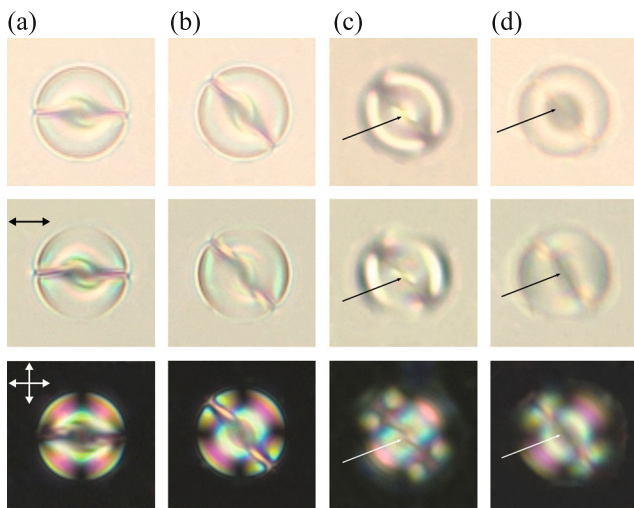
Fig. 2. (Color online) Photographs of the droplet with the toroidal cholesteric structure when the axis of symmetry of the droplet lies in the plane of the composite film and (a) is perpendicular to the polarizer and (b–d) makes an angle of 45° with the polarizer when the microscope is focused (b) on the center of the droplet and (c, d) on the segment of the ring defect (c) above and (d) below the center of the droplet. Photographs are taken in (upper panels) unpolarized light, (middle panels) in the scheme with a switched-off analyzer, and (lower panels) in crossed polarizers. Single arrows indicate the position of the ring defect. The diameter of the droplet is 11 μm.

we calculated the distribution of the cholesteric wave vector $\mathbf{q(r)}$ whose direction coincides with the local direction of the axis of the cholesteric helix by interpo-

lating the local director field by an unperturbed cholesteric helix. At each mesh point, we calculated the pitch of the helix $2\pi/|\mathbf{q}|$ and the direction of the twist vector $\mathbf{q}/|\mathbf{q}|$ that provide the best description of the local director distribution taking into account 26 nearest neighbors. Figure 3b shows the principal cross sections of the field $\mathbf{q}$ thus obtained by the planes that pass through the axis of symmetry of the structure and are perpendicular to it. For convenience, the directions of the field are represented by unit vectors and $|\mathbf{q}|$ is shown by a color map (see the inset). Images of the toroidal structure of the cholesteric liquid crystal in crossed polarizers (Fig. 3c) calculated by the Jones matrix method [30] correspond to the experimentally observed pictures (Figs. 1a and 2a).

The homeotropic anchoring in cholesteric droplets promotes the formation of a structure with different magnitudes of the wave vector $|\mathbf{q}|$ in the bulk of the droplet. For the toroidal cholesteric structure, twist strains hardly exist in most of the bulk of the droplet. In particular, the relative magnitude of the wave vector $|\mathbf{q}|/|\mathbf{q}_0|$ is no more than 1/3 not only near the boundary of the droplet but also in the central region most distant from the interface (Fig. 3b). The twist strain is significant only near the ring defect, where the local pitch of the helix is close to the intrinsic pitch of the helix. In larger droplets (at large ratios d/p_0), the difference between the wave vectors of the cholesteric liquid crystal in the free state $\mathbf{q}_0$ and the wave vector $\mathbf{q}$ formed in the droplet is larger. This behavior fundamentally distinguishes this structure from the layered structure with the bipolar helix axis distribution [25], where the
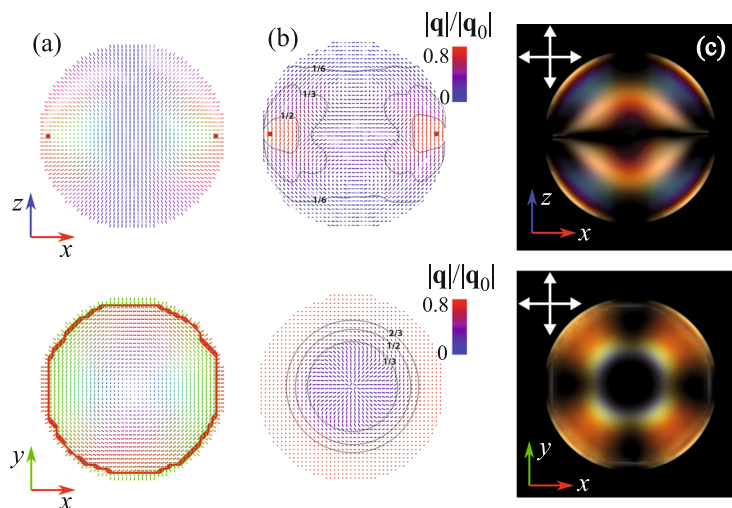

Fig. 3. (Color online) (a) Calculated configuration of the director in the droplet with the toroidal cholesteric structure with the surface ring defect in the central cross section. The director field distribution in the Ox, Oy, and Oz directions is shown in red, green, and blue, respectively. The thick red line marks the ring defect. (b) Wave vector field $\mathbf{q}$ of the cholesteric helix colored according to the relative magnitude $|\mathbf{q}|/|\mathbf{q}_0|$. Contours indicate the boundaries of the regions under the conditions $|\mathbf{q}|/|\mathbf{q}_0| < 1/6$, $|\mathbf{q}|/|\mathbf{q}_0| < 2/6$, and $|\mathbf{q}|/|\mathbf{q}_0| < 4/6$. (c) Simulated optical textures in the geometry of crossed polarizers. The diameter of the droplet is 1.8 μm.

period of the structure with an increase in the diameter of the droplet approaches the period of the cholesteric liquid crystal in the free state. In this case, the character of the wave vector distribution generally does not change with an increase in d/p_0, but contours (Fig. 3b) corresponding to $|\mathbf{q}|/|\mathbf{q}_0| = 1/6$, $2/6$, and $4/6$ are shifted toward the ring defect. Such a change in the relative magnitude of the wave vector is accompanied by an increase in the elastic strain energy, primarily twist strain energy. At the same time, the stability of the toroidal cholesteric structure with increasing d/p_0 can be explained by the existence of the ring surface defect whose relative length (length divided by the diameter of the droplet) and, thereby, the surface energy do not increase in the axisymmetric structure.

To conclude, we have revealed and studied in detail the axisymmetric toroidal structure in cholesteric droplets with the homeotropic boundary conditions. This structure is formed in cholesteric liquid crystal droplets at ratios $1.4 < d/p_0 < 2.9$, which are between the values characteristic of the twisted radial structure and the configuration with the bipolar helix axis distribution. The toroidal cholesteric structure is characterized by a surface ring defect, which is located in the equatorial plane and increases the contribution of the surface energy to the total free energy of the system. Thus, a change in the anchoring energy in cholesteric liquid crystals at the interface will affect the balance of energies associated with elastic strains and the length of the defect. In this case, the toroidal structure of cholesteric droplets can be highly sensitive to changes at the interface, which will allow the application of systems with such structures as highly sensitive sensors.

REFERENCES

1. P. Oswald and P. Pieranski, *Nematic and Cholesteric Liquid Crystals: Concepts and Physical Properties Illustrated by Experiments* (Taylor and Francis, Boca Raton, 2005).

2. G. E. Volovik, JETP Lett. **28**, 59 (1978).

3. M. Kleman and O. D. Lavrentovich, *Soft Matter Physics: An Introduction* (Springer, New York, 2003).

4. H.-S. Kitzerow, Liq. Cryst. **16**, 1 (1994).

5. Y. Geng, J.-H. Jang, K.-G. Noh, J. Noh, J. P. F. Lagerwall, and S.-Y. Park, Adv. Opt. Mater. **6**, 1700923 (2018).

6. M. Humar and I. Muševič, Opt. Express **18**, 26995 (2010).

7. G. Cipparrone, A. Mazzulla, A. Pane, R. J. Hernandez, and R. Bartolino, Adv. Mater. **23**, 5773 (2011).

8. G. Tkachenko and E. Brasselet, Nat. Commun. **5**, 3577 (2014).

9. J. Yoshioka, F. Ito, Y. Suzuki, H. Takahashi, H. Takizawa, and Y. Tabe, Soft Matter **10**, 5869 (2014).

10. J. Yoshioka and F. Araoka, Nat. Commun. **9**, 432 (2018).

11. T. Yamamoto and M. Sano, Soft Matter **13**, 3328 (2017).

12. F. Xu and P. P. Crooker, Phys. Rev. E **56**, 6853 (1997).

13. J. Bezic and S. Žumer, Liq. Cryst. **11**, 593 (1992).

14. Y. Zhou, E. Bukusoglu, J. A. Martínez-González, M. Rahimi, T. F. Roberts, R. Zhang, X. Wang, N. L. Abbott, and J. J. de Pablo, ACS Nano **10**, 6484 (2016).

15. Y. Bouligand and F. Livolant, J. Phys. (Paris) **45**, 1899 (1984).

16. S. Candau, P. le Roy, and F. Debeauvais, Mol. Cryst. Liq. Cryst. **23**, 283 (1973).

17. D. Seč, T. Porenta, M. Ravnik, and S. Žumer, Soft Matter **8**, 11982 (2012).

18. A. Darmon, M. Benzaquen, S. Čopar, O. Dauchot, and T. Lopez-Leon, Soft Matter **12**, 9280 (2016).

19. G. Posnjak, S. Čopar, and I. Muševič, Sci. Rep. **6**, 26361 (2016).

20. G. Posnjak, S. Čopar, and I. Muševič, Nat. Commun. **8**, 14594 (2017).

21. H.-S. Kitzerow and P. P. Crooker, Liq. Cryst. **13**, 31 (1993).

22. M. N. Krakhalev, A. P. Gardymova, O. O. Prishchepa, V. Yu. Rudyak, A. V. Emelyanenko, J.-H. Liu, and V. Ya. Zyryanov, Sci. Rep. **7**, 14582 (2017).

23. D. Seč, S. Čopar, and S. Žumer, Nat. Commun. **5**, 4057 (2014).

24. J. Pierron, V. Tournier-Lasserve, P. Sopena, A. Boudet, P. Sixou, and M. Mitov, J. Phys. II (France) **5**, 1635 (1995).

25. M. N. Krakhalev, A. P. Gardymova, A. V. Emel'yanenko, Jui-Hsiang Liu, and V. Ya. Zyryanov, JETP Lett. **105**, 51 (2017).

26. P. S. Drzaic, *Liquid Crystal Dispersions* (World Scientific, Singapore, 1995).

27. V. Yu. Rudyak, A. V. Emelyanenko, and V. A. Loiko, Phys. Rev. E **88**, 052501 (2013).

28. T. Orlova, S. J. Aßhoff, T. Yamaguchi, N. Katsonis, and E. Brasselet, Nat. Commun. **6**, 8603 (2015).

29. P. J. Ackerman and I. I. Smalyukh, Phys. Rev. X **7**, 011006 (2017).

30. R. Ondris-Crawford, E. P. Boyko, B. G. Wagner, J. H. Erdmann, S. Zumer, and J. W. Doane, J. Appl. Phys. **69**, 6380 (1991).

Translated by R. Tyapaev